$\gamma \rightleftarrows \varepsilon$ MARTENSITIC TRANSFORMATION IN Fe–Mn–Si ALLOYS

A. A. Gulyaev, E. Z. Vintaikin,
E. L. Svistunova, and A. B. Oralbaev

UDC 669.017.3:669.1'74'782

A study of the face-centered cubic (γ) $\rightleftarrows$ close-packed hexagonal (ε) transformation in manganese steels and alloys has been the subject of a number of works [1-3]. In them primary attention has been devoted to investigation of binary Fe–Mn alloys containing 18-22% Mn with a large volume share of ε-martensite. It is assumed that with an increase in manganese content in binary alloys above 22% the quantity of ε-martensite decreases and the $M_s^{\gamma\to\varepsilon}$ temperature drops.

According to the data of various authors with a 24-27% Mn content in the alloys (depending upon the purity of the investigated alloys) the $M_s^{\gamma\to\varepsilon}$ drops to 20°C and then to sublow temperatures so sharply even with an insignificant increase in Mn content in binary Fe–Mn alloys that it was practically impossible to experimentally clearly record the $M_s^{\gamma\to\varepsilon}$ in them in the area of negative temperatures. With addition of the majority of alloy elements (C, Ni, Cr, Mo, etc.) to Fe–Mn alloys $M_s^{\gamma\to\varepsilon}$ drops, which makes it possible to record in them a completely austenitic structure after hardening with lower Mn contents than in binary Fe–Mn alloys. An exception is silicon, additions of which to binary Fe–Mn alloys (with 20% Mn) either does not influence $M_s^{\gamma\to\varepsilon}$ [4] or increases it very weakly [2]. The rules given above are confirmed by investigation results [1-3] but there are factors which still have not found an appropriate explanation. For example, first, according to theoretical calculation of the phase diagram of Fe–Mn alloys by the method of approximation of regular solutions [5] the $M_s^{\gamma\to\varepsilon}$ temperature in alloys with 35-40% Mn is located close to 0°C, which is significantly above the experimental values. Second, in [6] a small quantity of ε-martensite (several percent) was observed in binary Fe–Mn alloys all the way to a content of 37% Mn in them by methods of nuclear gamma resonance and transmission electron microscopy. Third, an analysis of data on Fe–Mn–Si alloys developed at present [7, 8] with the memory of form effect containing about 30% Mn and up to 6% Si indicates a complex relationship of the $M_s^{\gamma\to\varepsilon}$ temperature of these alloys to the Mn and Si contents in them which does not agree with earlier obtained investigation results of alloys with lower Mn and Si contents (type G20S2) [1, 2, 4]. In connection with this in this work an investigation was made of the kinetic features of the $\gamma \to \varepsilon$-martensitic transformation in high-manganese binary and ternary (with silicon) alloys (Table 1).

TABLE 1

Alloy	Content of elements, %		M_s	M_f	A_s	A_f	T_N
	Mn	Si	°C				
G30	29,5	—	—	—	—	—	50
G30S1,5	28,9	1,5	—	—	—	—	100
G30S3	29,8	2,9	—25	—60	120	155	—65
G30S5,5	29,8	5,5	—35	—75	130	160	$\leqslant$—75
G26S5,5	25,9	5,3	+50	+15	160	185	$\leqslant$—100
G28S5,5	28,0	5,4	—10	—55	150	170	$\leqslant$—100
G32S5,5	31,9	5,3	—	—	—	—	$\sim$0
G34S5,5	33,7	5,5	—	—	—	—	$>$0

Note. The base of all of the alloys is iron.

I. P. Bardin Central Scientific-Research Institute for Ferrous Metallurgy. Chimkent Chemical Technology Institute. Translated from Metallovedenie i Termicheskaya Obrabotka Metallov, No. 8, pp. 8-10, August, 1991.

 0026-0673/91/0708-0574$12.50

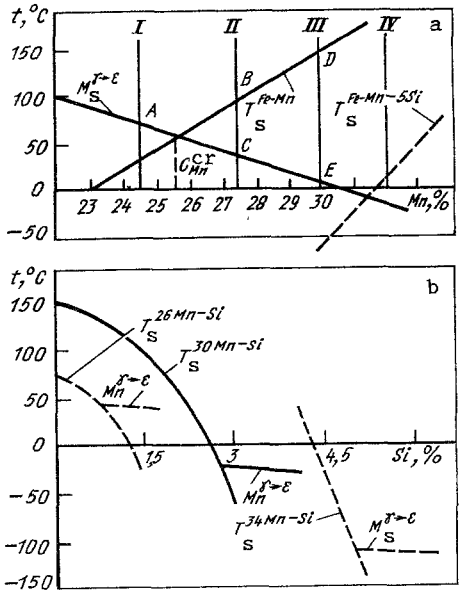

Fig. 1. The influence of manganese (a) and silicon (b) contents on the $M_s^{\gamma\to\varepsilon}$ and T_N temperatures in Fe–Mn and Fe–Mn–Si alloys (I-IV).

All of the alloys were melted in an open induction furnace, forged and rolled at 1100°C, and then specimens were cut from them and water hardened from 1000°C. The structures of the alloys were investigated on a Neophot-2 light microscope and a BS-540 electron microscope, the kinetics of the martensitic transformation and magnetic transition were investigated on a Sincoh-Ricoh dilatometer in the −196 to +300°C temperature range, and the x-ray diffraction analysis was made on a DRON-3 instrument in iron K_α-radiation.

The investigation results showed that all of the alloys except G26S5 have a completely austenitic structure while G26S5 has a two phase $\gamma + \varepsilon$ one. In the dilatometric investigations (taking into consideration literature data) the temperature ranges of the $\gamma \rightleftarrows \varepsilon$ martensitic transformation were established and the temperatures of the paramagnetic austenite → antiferromagnetic austenite transition (Neel points T_N) were determined. As follows from the data obtained, manganese reduces $M_s^{\gamma\to\varepsilon}$ and increases T_N while silicon reduces T_N and has a complex influence on $M_s^{\gamma\to\varepsilon}$, which basically agrees with literature data [1-6]. A characteristic feature of all alloys undergoing a martensitic transformation in cooling is observation of the condition $M_s^{\gamma\to\varepsilon} > T_N$, that is, the martensitic transformation occurs only in paramagnetic austenite. The martensitic transformation was not observed in the antiferromagnetic matrix ($M_s^{\gamma\to\varepsilon} < T_N$) in the investigated alloys, which agrees with the data of [6-8].

Let us consider the influence of silicon and manganese on $M_s^{\gamma\to\varepsilon}$ and T_N in detail. On the basis of experimental and literature data and also taking into consideration extrapola- of it into different concentrations of manganese and silicon the influence of these elements on the positions of the $M_s^{\gamma\to\varepsilon}$ and T_N points in Fe–Mn and Fe–Mn–Si alloys was determined. As may be seen from Fig. 1a, the $M_s^{\gamma\to\varepsilon}$ of the binary alloy G22 (∿100°C) decreases linearly with an increase in manganese content while in this case T_N increases. The meeting point of these curves, which occurs with a manganese concentration of C_{Mn}^{cr}, is peculiar to Fe–Mn alloys. With $C_{Mn} > C_{Mn}^{cr}$ the $\gamma \to \varepsilon$ martensitic transformation must occur in antiferromagnetic austenite ($T_N > M_s^{\gamma\to\varepsilon}$) but it is not observed experimentally. With $C_{Mn} < C_{Mn}^{cr}$ an $M_s^{\gamma\to\varepsilon}$ temperature dropping with an increase in C_{Mn} is observed on the dilatometric curves while with $C_{Mn} > C_{Mn}^{cr}$ the $\gamma \to \varepsilon$ transformation is not observed.

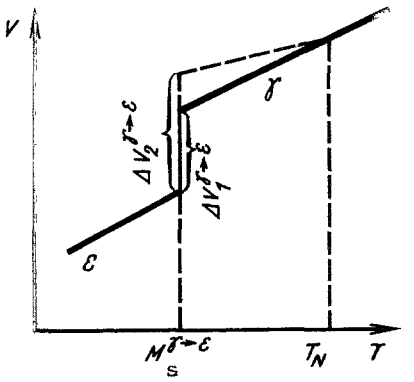

Fig. 2. Plan of volumetric changes during the $\gamma \to \varepsilon$ transformations with $T_N > M_s^{\gamma\to\varepsilon}$ ($\Delta V_2^{\gamma\to\varepsilon}$) and $T_N < M_s^{\gamma\to\varepsilon}$ ($\Delta V_1^{\gamma\to\varepsilon}$).

Therefore it may be stated that in the transformation of austenite from the paramagnetic to the antiferromagnetic condition the martensitic transformation closes in a jump. This agrees with the results of investigation of Fe–Mn–Si alloys given below and also with certain assumptions developed in [4, 6]. Stabilization of austenite in relation to the $\gamma \to \varepsilon$ martensitic transformation in transformation of austenite from the paramagnetic to the antiferromagnetic condition requires a special theoretical analysis and in first approximation may be explained by the composite action of the following factors. First, by decreasing the Gibbs free energy of austenite as the result of magnetic ordering. Second, by a possible increase in packing defect energy of austenite in formation of magnetic order [4]. Third, by strengthening of austenite in the transition into the antiferromagnetic condition [1] with subsequent more difficult movement of Shockley partial dislocations carrying out the $\gamma \to \varepsilon$ transformation. Fourth, by antiferromagnetic invariance of austenite (Fig. 2) including the fact that at temperatures below T_N the linear expansion of specimens increases with an increase in temperature more slowly than in the paramagnetic area [9], as the result of which the volumetric effect necessary for the $\gamma \to \varepsilon$ transformation increases.

Therefore with a certain manganese concentration C_{Mn}^{cr} in binary Fe–Mn alloys (which depending upon the purity of the alloys is 24-27%) the $M_s^{\gamma\to\varepsilon}$ temperature does not drop sharply as was assumed earlier and the $\gamma \to \varepsilon$ transformation itself closes in connection with the transformation of austenite into the antiferromagnetic condition. Using these assumptions it is possible to explain the above noted differences in the experimental and calculated data on the concentration relationship of $M_s^{\gamma\to\varepsilon}$ in the Fe–Mn system. In the calculations [5] the magnetic contribution to the equation for free energy of the alloy was not calculated and it was assumed that for all of the investigated C_{Mn}'s austenite is paramagnetic. In this case [if the $T_N = f(\%Mn)$ curve in Fig. 1a and closing of the $\gamma \to \varepsilon$ transformation with $C_{Mn} = C_{Mn}^{cr}$ are not taken into consideration] the $M_s = f(\%Mn)$ curve basically agrees with the calculated data that $M_s^{\gamma\to\varepsilon} \cong 0°C$ with $C_{Mn} > 30\%$.

As noted above, silicon has practically no influence on the $M_s^{\gamma\to\varepsilon}$ of Fe–Mn alloys. In this case, if the above discussions are not taken into considerations, it is impossible to explain, for example, the fact that G30 and G30S1.5 alloys are completely stable down to −196°C, the addition of even 1.5% Si (G30S3 alloy) immediately increases $M_s^{\gamma\to\varepsilon}$ to −25°C, but further alloying with silicon changes it very little. Similar kinetic features may be seen in analysis of literature data [6-8]. With the model proposed by us it is possible to easily explain these facts. With addition of silicon to Fe–Mn alloys there is a reduction in T_N (Fig. 1a, broken line) and the meeting point is shifted in the direction of lower temperatures and higher manganese concentrations (in Fig. 1a it is assumed that $M_s^{\gamma\to\varepsilon}$ is completely independent of C_{Si}).

Taking into consideration the proposed model let us consider the phase transformations in the four alloys I-IV with different manganese contents (Fig. 1a). In cooling alloy I

undergoes the $\gamma \rightarrow \varepsilon$ transformation at point A, alloy II undergoes the magnetic transformation at point B and stabilizes (does not transform) in relation to the possible martensitic transformation at point C, alloy III also undergoes the magnetic transformation at point D but in alloying of it with silicon and a corresponding reduction in T_N below $M_s^{\gamma\rightarrow\varepsilon}$ the martensitic transformation occurs at point E, and, finally, alloy IV (both with and without silicon) does not experience the martensitic transformation since in both cases $T_N > M_s^{\gamma\rightarrow\varepsilon}$. The interrelationship of the magnetic and martensitic transformations for Fe–Mn–Si alloys is shown in Fig. 1b. It may be seen that with $T_N > M_s^{\gamma\rightarrow\varepsilon}$ the transformation closes while, on the other hand, if $M_s^{\gamma\rightarrow\varepsilon} > T_N$ the transformation becomes possible and with an increase in silicon content there is practically no change in the M_S point.

The model proposed by us and the plans shown in Fig. 1 make it possible to completely explain the data on the kinetics of the magnetic and martensitic transformations in Fe–Mn–Si alloys. These alloys possess the memory of form effect and therefore it is important that quenching martensite, which reduces the memory of form effect, either does not form at all ($T_N > M_s^{\gamma\rightarrow\varepsilon}$) with the optimum manganese content ($\sim$30%) and addition of silicon or forms at temperatures somewhat below 0°C (Fig. 1b). In this case the deformation forming the memory of form effect prescribed at 20°C leads to formation of stress martensite of a single orientation, which has a favorable influence on the memory of form effect.

It should be noted that data on the presence of a small quantity of ε-martensite in alloys with $T_N > M_s^{\gamma\rightarrow\varepsilon}$ [6] in principle contradicts the above presented assumptions. In our experiments conducted on G30 binary and G32S5 and G34S5 ternary alloys with $T_N > M_s^{\gamma\rightarrow\varepsilon}$ it was also possible to observe individual fine crystals of ε-martensite on the electron microscope. In [6] this is explained by the fact that if the thickness of ε-martensite crystals does not exceed some critical dimension (several nm) from the assumptions of magnetic and thermodynamic theories [10] such paramagnetic areas may be formed in the antiferromagnetic matrix and closing of the martensitic transformation occurs only upon these crystals reaching a critical size. While not denying the possibility of such an explanation as an alternative point of view, it may be assumed that the reason for formation of these crystals is the stresses occurring in hardening of the specimens or preparation of foils for electron microscopic investigation. Taking into consideration the low values of the motive force $\Delta G^{\gamma\rightarrow\varepsilon}$ and the broad $M_s^{\gamma\rightarrow\varepsilon}$–$M_d^{\gamma\rightarrow\varepsilon}$ temperature range for the $\gamma \rightarrow \varepsilon$-transformation and also, apparently, the small additional barrier caused by antiferromagnetic ordering the occurrence of even insignificant stresses at a temperature significantly above $M_s^{\gamma\rightarrow\varepsilon}$ but below $M_d^{\gamma\rightarrow\varepsilon}$ may lead to formation of individual crystals of stress or deformation ε-martensite in alloys with $T_N > M_s^{\gamma\rightarrow\varepsilon}$ (in our experiments G30, G32S5, and G34S5).

LITERATURE CITED

1. I. N. Bogachev and V. F. Egolaev, The Structure and Properties of Iron-Manganese Alloys [in Russian], Metallurgiya, Moscow (1973).
2. O. G. Sokolov and K. B. Katsov, Iron-Manganese Alloys [in Russian], Naukova Dumka, Kiev (1982).
3. L. I. Lysak and B. I. Nikolin, Physical Fundamentals of the Heat Treatment of Steel [in Russian], Tekhnika, Kiev (1975).
4. I. N. Bogachev and G. E. Zvigintseva, "The influence of the magnetic condition of austenite on the martensitic transformation," Dokl. Akad. Nauk SSSR, 215, No. 3, 570-571 (1974).
5. J. F. Breedis and C. Kaufman, "Formation of HCP and BCC phases in austenitic iron alloys," Metall. Trans., 2, No. 9, 2359-2371 (1971).
6. E. Gartstein and A. Rabinkin, "On the FCC-HCP phase transformation in high manganese–iron alloys," Acta Metall., 27, No. 6, 1053-1064 (1979).
7. M. Sade, K. Halter, and E. Hornbogen, "The effect of thermal cycling on the transformation behaviour of Fe–Mn–Si shape memory alloys," Z. Metallkunde, 79, No. 8, 487-491 (1988).
8. A. Sato, Y. Yamaji, and T. Mori, "Physical properties controlling shape memory effect in Fe–Mn–Si alloys," Acta Metall., 34, No. 2, 287-294 (1986).

9. V. L. Sedov, The Antiferromagnetism of γ-Fe. The Problem of Invar [in Russian], Nauka, Moscow (1987), pp. 83-85.
10. L. Neel, J. Phys. Soc. Jpn., 17, No. 4, 676-681 (1962).

FEATURES OF OXIDATION OF Ni—Cr ALLOYS WITH ADDITIONS OF Sc AND Y

G. S. Braslavskaya and
S. B. Maslenkov

UDC 621.78.019.82:669.245

The mechanism of formation of scale on Ni—Cr alloys was established with use of X-ray diffraction analysis and other modern methods. It was shown that in the 700-1200°C range in the initial stage of oxidation single-layer Cr_2O_3 scale is formed on Ni—Cr alloys with and without additions of rare-earth metals. In further oxidation the structure of the oxide layer depends significantly upon the annealing temperature and time. With addition of rare earth metals an effect similar to the reduction in oxidation temperature is observed; the time of existence of the single-phase scale increases. In this case the oxidation rate of the alloys drops by several times.

The mechanism of formation of scale on nickel—chromium alloys has been studied and described in many experimental works. In the initial moments of oxidation the formation of both equilibrium Cr_2O_3 oxide in contact with the Ni—Cr alloy and nonequilibrium NiO oxides and $NiCr_2O_4$ spinel was observed [1]. With oxidation a continuous Cr_2O_3 oxide layer is formed at the metal—scale interface. As is assumed at present, this plays a determining role in the pro tective properties of alloys containing more than 10% Cr.

Micro-x-ray spectral analysis [1-3] established the rule of formation of scale characteristic of both nickel and iron alloys: Oxide phases formed in the heterophase scale of alloys are located in it not randomly but in the form of individual layers. According to the plan proposed by the author of [4] basically for NiCr-alloys the phase composition of the oxide film in relation to oxidation temperature may be represented in the form of the following model (Table 1).

In investigations of subsequent years ([5] for example) it was shown that the phase composition of the scale changes with an increase in its thickness (Table 2).

Therefore it was established that protective films of three types are formed on Ni—Cr alloys. However, until now there has not been an explanation of the formation of different structures and primarily of the reasons for the change from one structure to another with a change in oxidation temperature and time.

It should be noted that the results of a number of experimental works contradict formation of the model of [4]. In the initial stage of oxidation at 950°C [6] and 1000°C [7] only

TABLE 1

t, °C	Layer-by-layer structure of the scale
500—700	Cr_2O_3
800—1000	Cr_2O_3, $NiCr_2O_4$
1000	Cr_2O_3; $NiCr_2O_4$, NiO

Note. The structure of the scale was determined on specimens of Ni-20% Cr alloy [4].

A. A. Baikov Institute of Metallurgy. Scientific-Research Institute for Nondestructive Testing. Translated from Metallovedenie i Termicheskaya Obrabotka Metallov, No. 8, pp. 10-15, August, 1991.

 0026-0673/91/0708-0578$12.50